ISSN: 2710-0588

Fractal Characteristics of Different Tectonic Coals in the Yuwu Mining Area based on Mercury Intrusion Porosimetry

Haodi Chang

SCHOOL OF RESOURCES AND ENVIRONMENT, HENAN POLYTECHNIC UNIVERSITY, Jiaozuo, Henan, China

Abstract

Tectonic coal is a product of intense deformation and transformation of coal under tectonic stress. The complexity of its pore structure directly affects the occurrence and migration efficiency of coalbed methane (CBM), which is one of the key factors restricting CBM development in high-stress mining areas. Located in the northeastern part of the Qinshui Basin, the Yuwu Mining Area is characterized by frequent regional tectonic activities, with various tectonic types such as faults and folds developed, resulting in the extensive distribution of tectonic coal and significant differences in metamorphic degree within the mining area. As an effective tool for quantifying the structural complexity of porous media, fractal theory has been widely applied in the characterization of coal pore structure. In this study, different types of tectonic coals (e.g., cataclastic coal, mylonitic coal) in the Yuwu Mining Area were selected as research objects. Combining low-temperature nitrogen adsorption experiments with the FHH fractal model, the fractal dimension characteristics of coal samples under different tectonic deformation intensities were systematically analyzed. The influence mechanism of tectonic activity on the fractal properties of coal pores was revealed, and the intrinsic correlation between fractal dimensions and pore structure parameters (specific surface area, pore volume, pore size distribution) was clarified. The research results can provide theoretical basis and data support for CBM reservoir evaluation and development plan optimization in the Yuwu Mining Area, while enriching the geological understanding of fractal evolution of tectonic coal pores.

Keywords

Mercury Intrusion Porosimetry, Fractal Theory, Pore Structure.

1. Introduction

As a foundational energy source in China's energy structure, coal accounts for approximately 65% of the total primary energy consumption. It will remain the dominant energy type for a fairly long period in the future[1]. In 2023, coal consumption accounted for about 55.3% of the total energy consumption, indicating that coal plays a crucial role in China's energy mix. In 2024, China's total primary energy output reached 4.98 billion tons of standard coal, among which raw coal output hit as high as 4.78 billion tons; the total energy consumption stood at 5.96 billion tons of standard coal, with coal consumption accounting for 53.2%[2].

Coal and gas outburst remains one of the major challenges in safety prevention and control within China's coal industry[3]. As a severe mining disaster, coal and gas outburst incidents occur suddenly in a short period[4]. During such accidents, massive amounts of coal are ejected and large volumes of gas gush out in stope or roadway spaces, generating intense dynamic effects that cause facility damage and casualties among underground workers. In severe cases, it may lead to airflow reversal, which in turn triggers secondary disasters such as gas explosions

ISSN: 2710-0588

and expands the scope of casualties. Coal and gas outburst thus poses a significant threat to coal mine safety production[5].

To address this critical threat, China has invested substantial research resources, gradually establishing a systematic and scientific theoretical system as well as prevention and control technologies[6]. These research findings and control measures have largely effectively curbed the occurrence of coal and gas outburst accidents in mines, significantly reduced accident risks, and provided strong support for safeguarding the lives of practitioners[7].

Based on the differences in pore and fracture structures of coal induced by varying tectonic deformation effects, and building on existing research achievements, this study employs experimental methods including high-pressure mercury intrusion porosimetry to investigate the controlling effects of different tectonic deformation degrees on the outburst potential and kinetic energy of coal. It further deepens the exploration of the evolution law of gas expansion energy in tectonically deformed coal and reveals the energy evolution mechanism underlying the outburst of such coal. This research is expected to provide a theoretical basis for improving the study on the energy mechanism of coal and gas outburst, and offer certain theoretical guidance for outburst prevention in mine excavation.

2. Mine Overview and Sample Collection

2.1. Mine Overview

Yuwu Coal Mine is located in the southeast of Shanxi Province, on the western side of Lu'an Mining Area, with the specific longitude and latitude ranging from 112°47′E to 112°54′E and 36°15′N to 36°25′N.

The mine is accessible via multiple transportation means including railways and highways. By railway, coal can be transported northward to Taiyuan, Shuozhou and other regions, and southward to Luoyang, Nanyang and beyond. Wuyang Railway Station, which is on the route, is 16 km away from the mining area, providing convenient conditions for coal trading and transportation. For long-distance transportation, the mine's railway is directly connected to major cities such as Taiyuan, Jiaozuo and Handan, with the longest haul distance reaching approximately 240 km. The coal loading and unloading station of the mining area is less than 30 km away from Changzhi North Railway Station, through which coal shipments bound for Handan can be dispatched or received.

In terms of highway transportation, the mining area is adjacent to National Highways G208 and G309, with dedicated mine roads linking to these two highways. Coal transported to Taiyuan can be delivered via the Taiyuan-Changzhi Expressway. Additionally, the mine's dedicated railway line is connected to the national railway network, enabling coal transportation across the entire country. The overall transportation conditions are thus highly convenient.

2.2. Analysis of Basic Sample Parameters

Table 1. Basic Analysis of Coal Samples

Coal Samples	Proximate Analysis			$R_{o,max}$/%
	M_{ad}/%	A_{ad}/%	V_{ad}/%	
YS	0.89	13.19	11.20	2.20
SE	0.92	6.50	10.45	2.30
SI	0.87	7.57	10.67	2.26
ML	0.84	4.76	10.82	2.12

Note: M_{ad} refers to moisture content on air-dried basis;A_{ad} refers to ash content on air-dried basis; V_{daf} refers to volatile matter content on dry ash-free basis; $R_{o,max}$ refers to maximum vitrinite reflectance.

ISSN: 2710-0588

In this study, coal samples collected from the Yuwu Mining Area were selected as the research objects. Proximate analysis and maximum vitrinite reflectance measurement were conducted separately on four types of tectonically deformed coal, namely primary structure coal (YS), cataclastic coal (SE), granular coal (SI) and mylonitic coal (ML). The basic parameters are presented in Table 1.

3. Pore Structure Characteristics of Coal Samples from Yuwu Mining Area

Coal is a porous medium, and its abundant internal nanopores make it a favorable structure for methane accumulation. The heterogeneity and connectivity of pore structures are key factors affecting gas adsorption and migration, which thus necessitate refined quantitative evaluation. In recent years, various advanced technologies have been applied to characterize the nanopore structures of coal, including scanning electron microscopy (SEM)[8], transmission electron microscopy (TEM)[9], low-pressure nitrogen adsorption (LP-N_2A)[10], low-pressure carbon dioxide adsorption (LP-CO_2A)[11], mercury intrusion capillary porosimetry (MICP)[10], nuclear magnetic resonance (NMR)[12], and Electromagnetic radiation[7]. This chapter characterizes the pore structures of tectonically deformed coal via high-pressure mercury intrusion experiments and investigates their evolutionary characteristics. With reference to the nanopore classification standards proposed by IUPAC, pores within the size range of 50–10000 nm are selected as the research focus, and an in-depth study on these nanopores is presented in this chapter.

3.1. Testing Theory and Methodology of Pore Structure

The experimental instrument employed for mercury intrusion porosimetry (MICP) was the AutoPore Ⅳ 9505 fully automatic mercury porosimeter manufactured by Micromeritics Instrument Corporation, USA. The coal samples used for the experiment were required to have a particle size of 3–6 mm. The coal samples were dried in a constant temperature oven at 70–80 °C for 12 hours, and after cooling to room temperature, the pore structure test of macropores in coal was conducted in accordance with GB/T 21650.1-2008 Determination of pore size distribution and porosity of solid materials by mercury intrusion porosimetry and gas adsorption methods.

As a non-wetting liquid, mercury is difficult to penetrate into the pore structure of coal under natural conditions (without external pressure application). However, when external pressure is applied to liquid mercury, this pressure can effectively overcome the resistance caused by the surface tension of mercury. During the process of continuous pressure increase, the relationship curve between pressure and mercury intrusion volume can be obtained through testing, and the pore size distribution characteristics and specific surface area distribution of coal samples can be further analyzed and derived with the help of this curve.[13] In addition, based on the Washburn equation applicable to cylindrical pores, the mathematical relationship between pressure p and pore diameter r can be deduced as follows:

$$d = \frac{-4\gamma\cos\theta}{p_c} \tag{1}$$

d is the radius of the cross-sectional circle of cylindrical pores, in nm; γ is the surface tension of mercury, taking a value of 0.480 N/m; θ is the contact angle of mercury on the sample, with a value of 140∘; p is the applied pressure, in MPa[14]. The pore size range tested by mercury intrusion porosimetry (MICP) in this study is 50–10000 nm.

The macropore morphologies can be basically classified into three types: open pores, semi-closed pores, and narrow-necked pores[15]. Among these, the distribution of open pore

ISSN: 2710-0588

channels is most favorable for gas migration, while that of closed pore channels is the least favorable, with transitional types falling between the two extremes. For coal with closed pore channel distribution, pores are mainly concentrated in the micropore range, resulting in poor gas migration pathways and increased migration resistance. Under such conditions, even if a large amount of gas is stored in the coal, it is difficult to escape effectively, which tends to form local high-pressure zones. Therefore, high risks of coal and gas outburst still exist during the mining of such coal seams, posing significant potential safety hazards[16].

The mercury intrusion-extrusion curves of coal can reflect pore characteristics, including pore size distribution, connectivity, and morphological features[17]. A comprehensive and direct analysis of coal pore characteristics can be achieved by characterizing mercury intrusion curves. According to the morphology of mercury intrusion hysteresis loops, the coal samples collected from the study area can be divided into two categories.

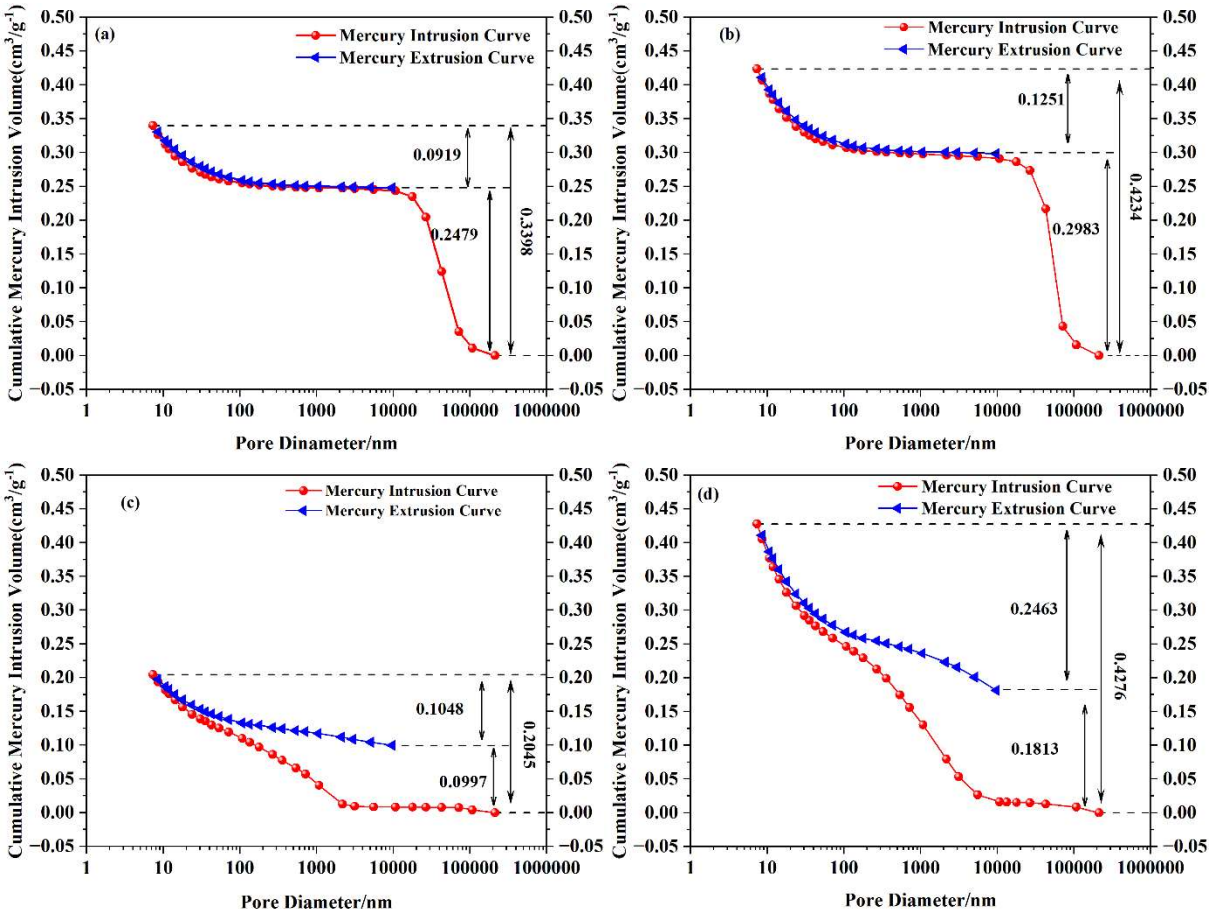

Fig. 1 Mercury Intrusion-Extrusion Curves of High-Pressure Mercury Intrusion Porosimetry

As shown in Fig. 1, samples a and b belong to Category Ⅱ, while samples c and d are categorized as Category Ⅰ. The mercury intrusion and extrusion curves of samples a and b are nearly parallel, with indistinctly developed hysteresis loops. Their dominant pore type is semi-closed pores, and the pore morphologies are mostly cylindrical or V-shaped, which are favorable for mercury extrusion. In contrast, samples c and d exhibit a rapid increase in mercury intrusion at the initial stage, indicating well-developed macropores and mesopores (including fractures), along with relatively distinct mercury extrusion hysteresis loops.

No obvious inflection points are observed in the extrusion curves of all four samples, a characteristic that suggests a low content of narrow-necked pores within the pore size range measured by mercury intrusion porosimetry. Significant differences are found in the total

ISSN: 2710-0588

mercury intrusion volumes among the four samples. Specifically, samples b (cataclastic coal) and d (mylonitic coal) show relatively high intrusion volumes, exceeding 4.2 cm^3/g. This is followed by sample a (primary structure coal) with an intrusion volume of 0.3398 cm^3/g, while sample c (granular coal) has the lowest intrusion volume of 0.3398 cm^3/g.

The differences in mercury extrusion volumes are also extremely pronounced. Sample d (mylonitic coal) has the maximum extrusion volume of 0.2463 cm^3/g, followed by sample b (cataclastic coal) with 0.1251 cm^3/g. Finally, the extrusion volumes of sample a (primary structure coal) and sample c (granular coal) are comparable, reaching 0.0919 cm^3/g and 0.1048 cm^3/g, respectively. The extrusion volume of sample d is 2.68, 1.97, and 2.35 times those of samples a, b, and c, respectively.

3.2. Macropore Volume-Specific Surface Area Characteristics

Fig. 2 illustrates the variation of macropore volume of coal samples with pore size distribution. The cumulative pore volume and incremental pore volume of the samples exhibit distinct evolutionary characteristics, respectively. For samples a and b, the pore volume shows a prominent peak at 6000 nm, and both the incremental and cumulative pore volume curves are extremely smooth within the study pore size range. In contrast, samples c and d present a distinct pore volume peak at 1000 nm, with relatively fluctuating incremental pore volume curves.

Combined with the findings in Section 3.2, the mercury extrusion characteristic curves of coal samples reveal that the discharge of residual mercury increases continuously with the decrease of pressure gradient, whereas the overall mercury extrusion efficiency remains relatively low. This result strongly suggests that semi-closed or closed secondary pores are widely distributed in the macropore and mesopore systems of coal samples. These pores exert a significant confinement effect on mercury, making it difficult to be completely expelled under low-pressure conditions[18].

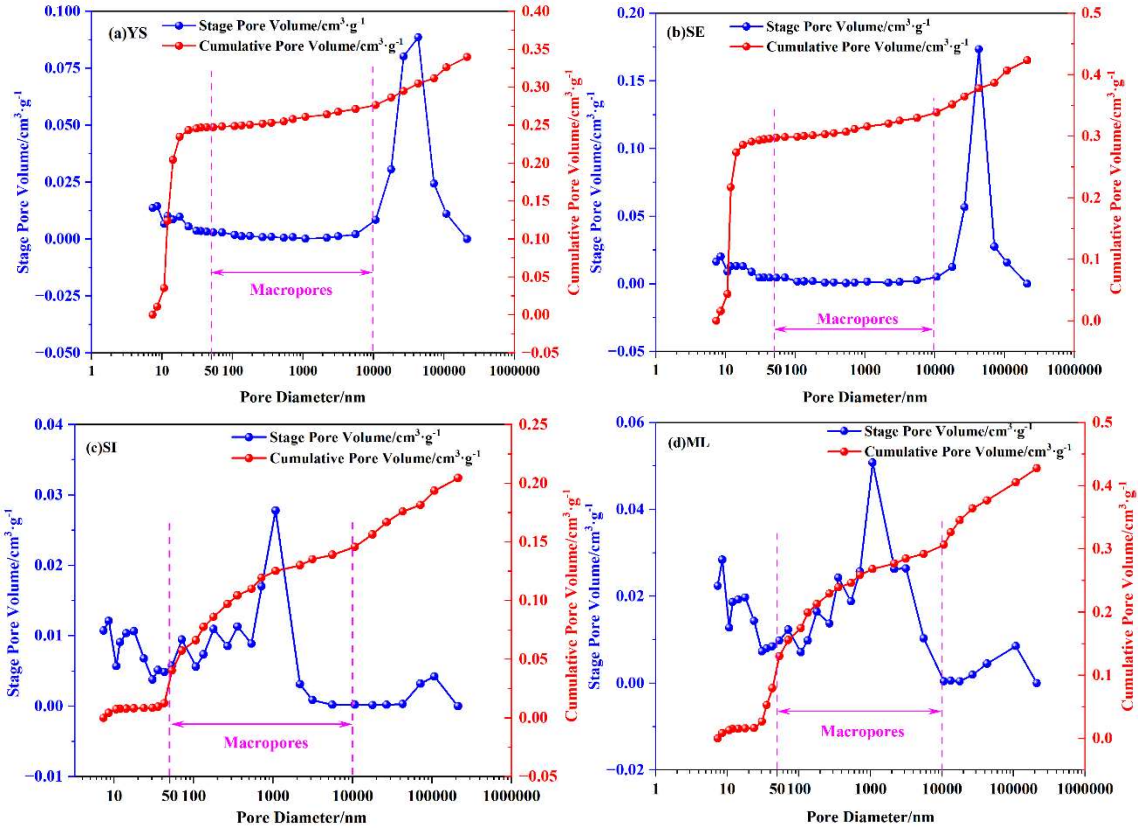

Fig. 2 Distribution of Macropore Volume versus Pore Size

ISSN: 2710-0588

Fig. 3 presents the distribution characteristics of macropore specific surface area of coal samples varying with pore size. The cumulative macropore specific surface areas of the four coal samples are 0.00862 $m^2 \cdot g^{-1}$, 0.00524 $m^2 \cdot g^{-1}$, 0.00019 $m^2 \cdot g^{-1}$ and 0.00022 $m^2 \cdot g^{-1}$, respectively. On the whole, no obvious variation trend is observed, but the cumulative macropore specific surface areas of samples a and b are significantly higher than those of samples c and d, with the difference exceeding one order of magnitude (i.e., 10 times).

It is worth noting that the incremental specific surface area of each coal sample exhibits a consistent variation pattern: it first decreases sharply and then tends to stabilize, eventually approaching zero gradually.

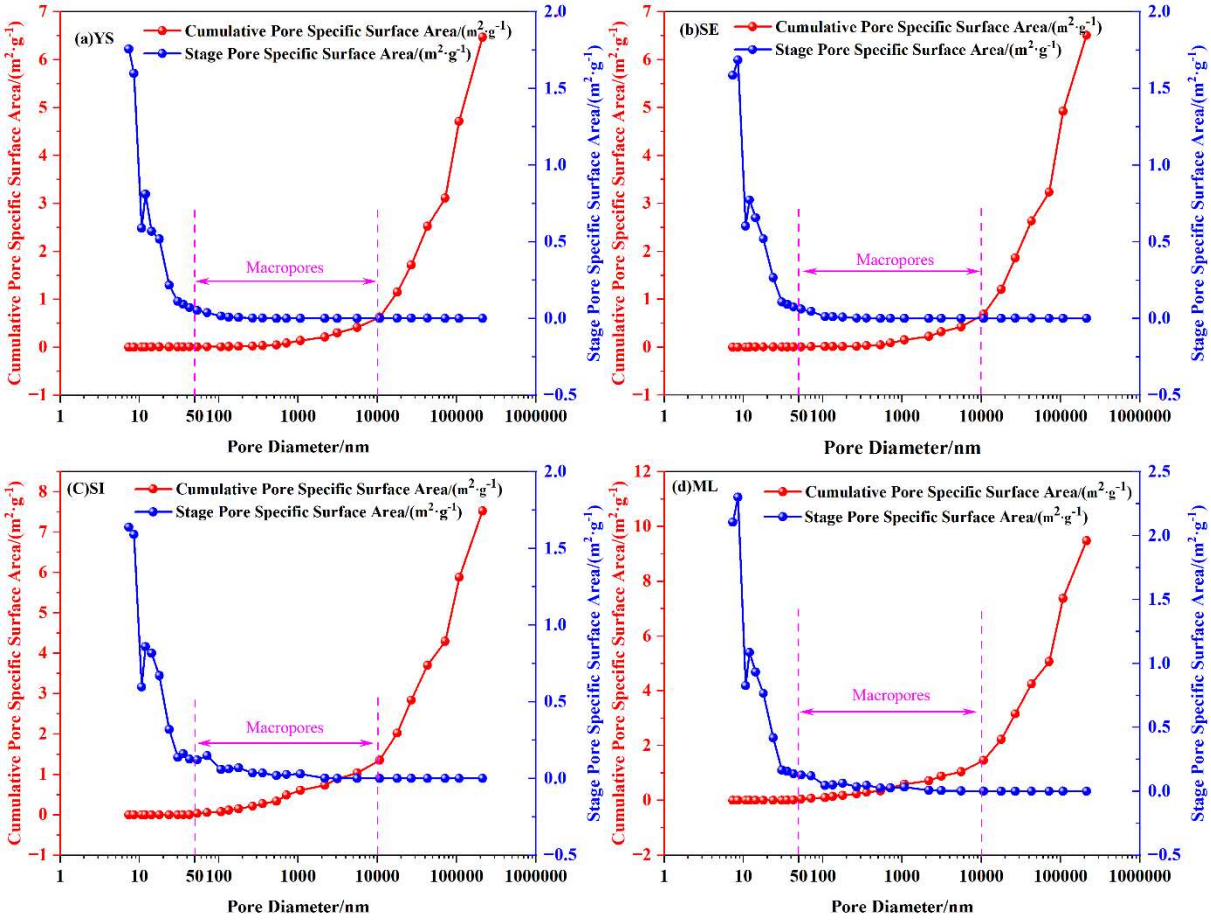

Fig. 3 Distribution of Macropore Specific Surface Area versus Pore Size

4. Fractal Characteristics of Pore Structure

4.1. Monofractal Characteristics of Pore Structure

Fractal dimension is a key quantitative parameter for characterizing the irregularity and complexity of coal pore structures, and its value directly reflects the characteristic differences of pore structures[19]. Mercury intrusion porosimetry (MICP) follows the principle of non-wetting capillarity during the mercury intrusion process, and the equilibrium relationship of mercury intrusion is expressed by the Washburn equation[20]. As a typical non-wetting liquid, the penetration behavior of mercury in pores complies with this physical law . The core value of the equation lies in establishing a quantitative correlation between pressure and pore size; the specific pore diameter parameters of porous media such as coal can be inversely calculated by measuring the mercury intrusion pressure, as shown below:

ISSN: 2710-0588

$$p = -2\sigma \cos \beta / r \tag{2}$$

p is the mercury intrusion pressure, in MPa; σ is the surface tension of mercury, generally taken as 0.485 N/m; β is the contact angle between mercury and the coal matrix, with a value of 130∘; r is the pore diameter, in nm. To further analyze the complexity of pore structures, the Menger sponge model was employed to establish the fractal characteristic equation for porous media[21]. Based on this model, the relationship between the mercury volume change rate and fractal dimension during the mercury intrusion process is expressed as follows:

$$\ln V_{Hg} = K_1 \ln(P_{Hg} - p_t) + const \tag{3}$$

V_{Hg} is the mercury intrusion volume, in cm^3/g; $K1$ is the fitting slope of mercury intrusion porosimetry; p_{Hg} is the mercury intrusion pressure, in MPa; pt is the initial mercury intrusion pressure, in MPa. The mercury intrusion volume and pressure obtained from the mercury intrusion experiment were subjected to logarithmic transformation for fitting. According to Equation (4), there is a linear relationship between $\ln V_{Hg}$ and $\ln(p_{Hg}-pt)$, and thus the relational expression between the fractal dimension D1 and the fitting slope K1 can be derived as follows:

$$K_1 = 3 - D_1 \tag{4}$$

As shown in Fig. 4, the scatter plot of $\ln V_{Hg}$ versus $\ln(p_{Hg}-pt)$ is plotted. According to Fig. 4, the pore structures in the range of 50–10000 nm of the four tectonically deformed coal samples exhibit distinct monofractal characteristics. The pore fractal dimensions are listed in Table 1; the macropore fractal dimensions of the four coal samples are 2.98919, 2.8717, 2.39314, and 2.49583, respectively. It can be observed that the fractal dimensions of tectonically deformed coal are significantly higher than those of raw coal, indicating that the macropore structure of raw coal is more complex.

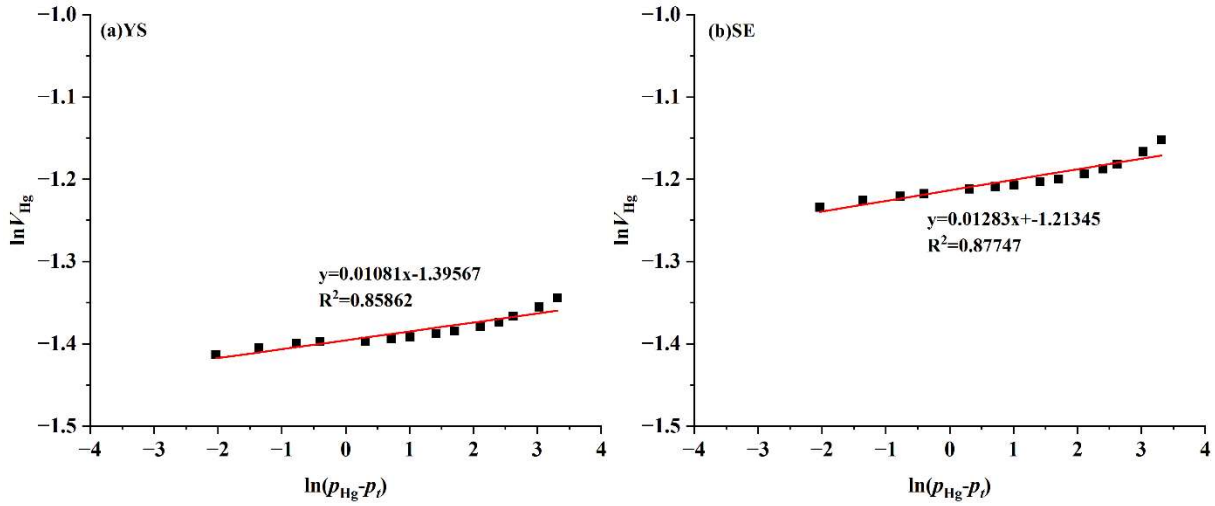

ISSN: 2710-0588

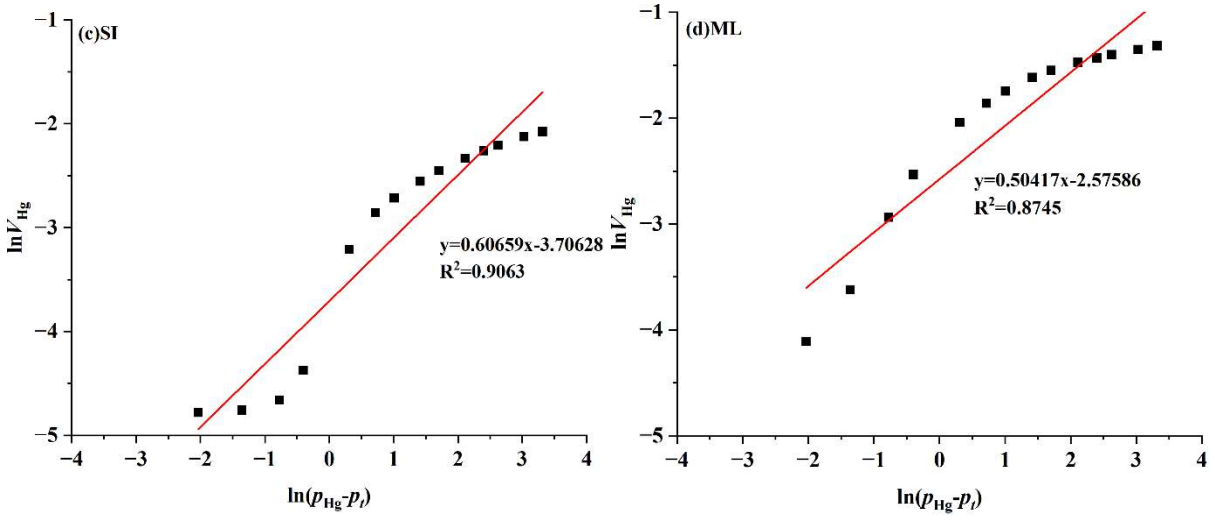

Fig. 4 Fitting Lines of Macropore Multifractal Dimensions of Coal Calculated Based on MIP Experimental Data

Table 2. Fractal Dimensions of Pores from Mercury Intrusion Porosimetry

Sample Number	Fitting Equation	Goodness of Fit R^2	Slope of the Equation K_1	Fractal Dimension D_1
YS	y=0.01081x-1.39567	0.85862	0.01081	2.98919
SE	y=0.01283-1.21345	0.87747	0.01283	2.8717
SI	y=0.60659x-3.70628	0.9063	0.60659	2.39314
ML	y=0.50417x-2.57586	0.8745	0.50417	2.49583

4.2. Multifractal Characteristics of Macropores

With an interval of q=1 across the continuous range of q=-10 to 10, the fitting curves of the partition function lg(q, ε) and scale ε for macropores of the four coal samples exhibit a significant strong linear relationship (Fig. 5), indicating that the macropores of coal samples have distinct multifractal characteristics[21]. Specifically, when q < 0, the fitting curves of the partition function show negative slopes. When q > 0, the fitting curves not only present obvious positive linear slopes but also feature dense data points, reflecting that pore sizes are concentrated in the small-scale interval of the characterized pore size range.Notably, the double logarithmic curves of the ML sample are relatively sparse, implying that the macropore size distribution of this sample has more significant differences within the corresponding scale rang[22].

ISSN: 2710-0588

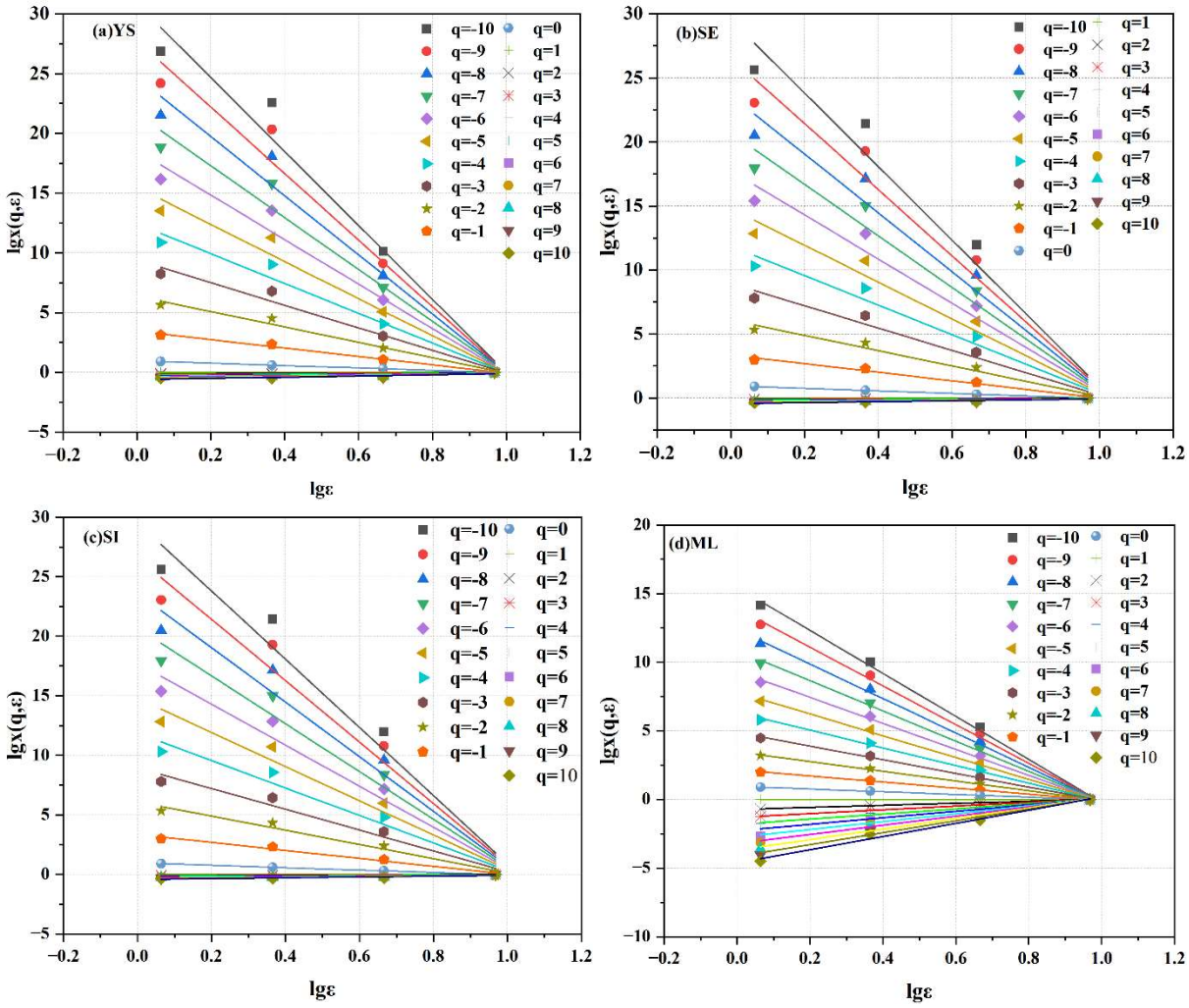

Fig. 5 lgε-lgμ(q, ε) Curves of Macropores

Fig. 6a presents the generalized fractal dimension curves of tectonically deformed coal from the Yuwu Mining Area. The generalized fractal dimensions Dq of macropores for the four coal samples exhibit a monotonically decreasing inverse S-shaped feature with the variation of q. When q<0,D in the low-probability measure domain decreases rapidly with the increase in q; when q>0, D q in the high-probability measure domain shows a slow downward trend as q increases.

Fig. 6b shows the mass exponent function curves of macropores in tectonically deformed coal from the Yuwu Mining Area. From the perspective of curve variation characteristics, the mass exponent function $\tau(q)$ of macropores in different tectonically deformed coal samples in this mining area shows a strictly increasing trend with the increase of parameter q, and generally exhibits an upward-convex nonlinear variation characteristic. On both sides of the critical value of q=0, the variation laws of the $\tau(q)$ curves are significantly different. Among them, the wide branch corresponding to q<0 is associated with the sparse zones of macropores in coal samples (i.e., the low-value zones of pore volume), reflecting the discrete distribution characteristics of macropores within this interval; while the narrow branch corresponding to q>0 corresponds to the dense zones of macropores (i.e., the high-value zones of pore volume), embodying the aggregated distribution characteristics of macropores in this interval[23].

A further analysis combined with the characteristics of the generalized fractal dimension curves in Fig. 6a shows that the variation patterns of both the mass exponent function τ(q) and the generalized fractal dimension spectrum D q for macropores of tectonically deformed coal

ISSN: 2710-0588

in the Yuwu Mining Area conform to the core judgment criteria of multifractals. On the one hand, τ(q) does not show a simple linear variation but exhibits an obvious nonlinear upward-convex trend, which is a typical characterization of multifractal structures at the level of the mass exponent function. On the other hand, the generalized fractal dimension D q presents an inverse S-shaped monotonically decreasing characteristic with the change of q, and shows different variation rates in the intervals of q<0 and q>0, which is highly consistent with the response law of fractal dimensions in different probability measure domains within the multifractal system.The above characteristics jointly confirm that the macropore structure of tectonically deformed coal in the Yuwu Mining Area has significant multifractal characteristics, reflecting the inhomogeneity and complexity of the macropores of tectonically deformed coal in this mining area in terms of scale distribution and spatial distribution[24].

The *Dq* curves intersect at the coordinate point (0,1), a characteristic indicating that the capacity dimension D0 of macropores, mesopores, and micropores in the coal samples takes a value of 1. A capacity dimension D0=1 implies that all types of pore subintervals contain valid pore volume data, with the Euclidean dimension of pore distribution being one-dimensional. This reflects the fundamental feature that pores in coal reservoirs exhibit a one-dimensional linear distribution on the spatial scale.

Further analysis of the numerical relationships among fractal dimensions reveals that the capacity dimension D0, information dimension D1, and correlation dimension D2 strictly follow the order of D0>D1>D2. This numerical characteristic demonstrates that the heterogeneity of pore structures across different scales in coal reservoirs cannot be described by a single fractal feature. The monofractal model only reflects the average fractal characteristics of pore structures and fails to capture the differential distribution laws of pores in different probability measure domains. In contrast, the multifractal model can accurately characterize the distribution characteristics of pores in sparse and dense zones through fractal dimensions of different orders, and thus is more suitable for representing the complex heterogeneity of pore structures in coal reservoirs.

This conclusion is highly consistent with the judgment that coal reservoir pores possess multifractal characteristics, which is derived from the analysis of lg(q,ε)−lgε double logarithmic curves. It mutually verifies the applicability and rationality of the multifractal model in characterizing the heterogeneity of coal reservoir pore structures from two perspectives: the numerical relationship of fractal dimensions and the analysis of curve morphology.

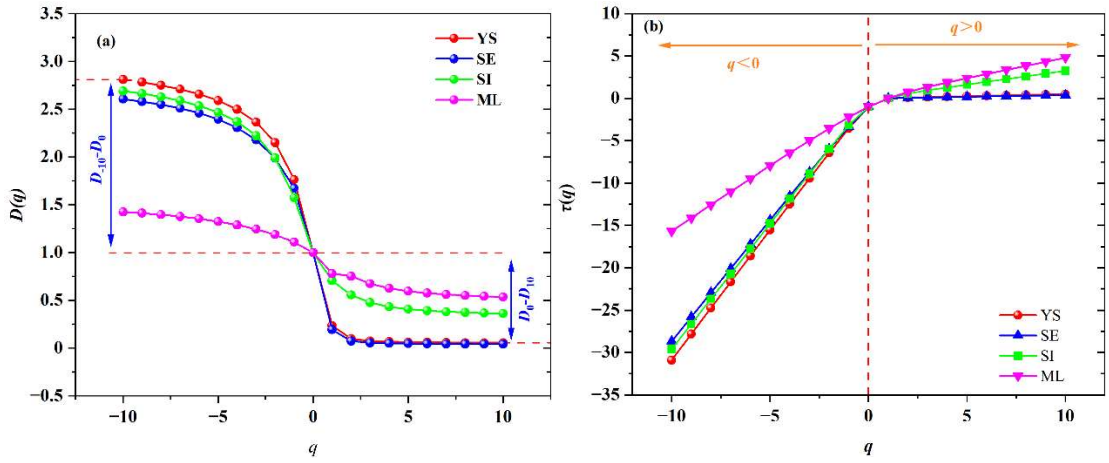

Fig. 6 Multifractal Curves of Macropores in Coal Samples; (a) Multifractal Dimension Spectrum *Dq* of Macropores (b) Statistical Moment Order q and Mass Exponent Function of Macropores

ISSN: 2710-0588

As shown in Fig. 7, the morphological characteristics of the multifractal singularity spectrum ($\alpha \sim f(\alpha)$) can also reveal the internal complexity and heterogeneity of the pore structure. The multifractal singularity spectra of all coal samples exhibit an inverted U-shaped distribution, where the $f(\alpha)$ values first increase and then gradually decrease with the rise of α, showing a typical convex function relationship. This result further confirms that the macropore structures of the coal samples all have significant multifractal characteristics[25].

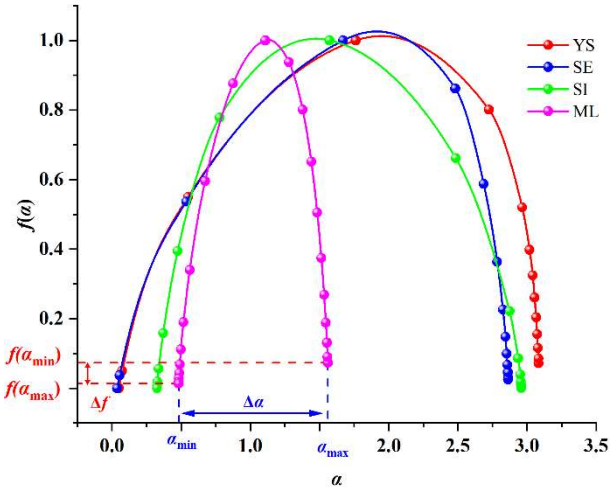

Fig. 7 Multifractal Singularity Spectrum of Macropores

Table 3. Multifractal Parameters of Macropores in Coal Samples from Yuwu Mining Area

Coal Sample	D_0	D_1	D_2	$\Delta(D_{-10}-D_0)$	$\Delta(D_0-D_{10})$	ΔD	α_0	$\Delta\alpha$	$\Delta f(\alpha)$
YS	1	0.2346	0.0979	1.8104	0.9453	2.7557	1.7631	3.0350	0.07187
SE	1	0.1922	0.0729	1.6061	0.9593	2.5655	1.6715	2.8277	0.02492
SI	1	0.1922	0.0729	1.6897	0.6382	2.3279	1.5732	2.6330	0.00071
ML	1	0.7794	0.7520	0.4253	0.4653	0.8906	1.1085	1.0780	0.05993

As can be seen from the data in the table, the D1 value of the ML coal sample from the Yuwu Mining Area is the largest, indicating that the macropore structure of this coal sample has the most significant singularity. The D1 values of the other three coal samples (YS, SE, SI) are relatively close, suggesting that the differences in their macropore singularity are small[26].

In terms of spectral width characteristics, the left spectral width Δ(D−10−D0) of the three coal samples (YS, SE, SI) is greater than the right spectral width Δ(D0−D+10), reflecting that the heterogeneity of the high-probability distribution regions of these three coal samples is stronger than that of the low-probability distribution regions. In contrast, the spectral width characteristics of the ML coal sample are the opposite, with the left spectral width smaller than the right spectral width.

From the perspective of total spectral width, the total spectral width of the three coal samples (YS, SE, SI) is greater than 2, indicating a high degree of singularity in their overall pore size distribution; the total spectral width of the ML coal sample is less than 1, suggesting a relatively low overall singularity. The above multifractal characteristics are all verified in the corresponding pore size distribution diagrams, confirming that the multifractal theory can provide an intuitive and quantitative characterization of the pore size distribution characteristics of coal samples. The overall curve morphologies also show significant differences, indicating extremely obvious differences in their pore structures.

α0 is the singularity value corresponding to fα(max); the larger its value, the stronger the local fluctuation of pore size distribution and the narrower the distribution interval. Δα is defined as

ISSN: 2710-0588

the difference between αmax and αmin; a larger value of this parameter reflects stronger heterogeneity in the pore size distribution of coal samples. Δf denotes the difference between fα(αmin) And fα(αmax), which can be used to characterize the relative proportion of small-volume pores and large-volume pores. When $\Delta f>0$, it indicates that pores in the low pore volume region exert a more significant influence on the overall pore size distribution.

5. Conclusion

Based on the research conducted, the following conclusions are drawn:

The coupled method of mercury intrusion porosimetry (MIP) and fractal theory exhibits significant effectiveness and unique advantages in the characterization of pore structures. By accurately obtaining the macropore structure characteristics of samples through MIP, the technical advantages of this method in the large pore size range are fully demonstrated. It makes up for the limitations of the adsorption method in macropore characterization, thereby forming a complete characterization system for the fractal characteristics of pores across a wide pore size range.

The macropore structure presents obvious multifractal characteristics, and the multifractal characteristic parameters can accurately describe the macropore structure features. This provides a solid theoretical basis for subsequent research.

References

[1] WEI Y, WANG Z, WANG H, et al. Compositional data techniques for forecasting dynamic change in China's energy consumption structure by 2020 and 2030 [J]. Journal of Cleaner Production, 2021, 284: 124702.

[2] QIAN W, ZHANG H, SUI A, et al. A novel adaptive discrete grey prediction model for forecasting development in energy consumption structure-from the perspective of compositional data [J]. Grey Systems: Theory and Application, 2021, 12(3): 672-97.

[3] LIU J, WANG K, ZOU J, et al. The implications of coal consumption in the power sector for China's CO2 peaking target [J]. Applied Energy, 2019, 253: 113518.

[4] CHANG S, ZHUO J K, MENG S, et al. Clean Coal Technologies in China: Current Status and Future Perspectives [J]. Engineering, 2016, 2: 447-59.

[5] YUE H, WU B, LI S, et al. Synergistic Optimization of Coal Power and Renewable Energy Based on Generalized Adequacy [J]. Applied Sciences, 2024, 14(17): 7864.

[6] LI W, ZHAO T, TU S. Experimental Study on Failure Characteristics and Energy Evolution Law of Coal–Rock Combination Body Under Different Quasi-Static Loading Rates [J]. Eng, 2025, 6(11): 287.

[7] WANG C, LI X, LIU L, et al. Dynamic effect of gas initial desorption in coals with different moisture contents and energy-controlling mechanism for outburst prevention of water injection in coal seams [J]. Journal of Petroleum Science and Engineering, 2023, 220: 111270.

[8] PAN J, ZHANG Z, LI M, et al. Characteristics of multi-scale pore structure of coal and its influence on permeability [J]. Natural Gas Industry B, 2019, 6(4): 357-65.

[9] LIU S, SANG S, WANG G, et al. FIB-SEM and X-ray CT characterization of interconnected pores in high-rank coal formed from regional metamorphism [J]. Journal of Petroleum Science and Engineering, 2017, 148: 21-31.

[10] ZHU J, SHAO T, LI G, et al. Multiscale Pore Structure Characteristics and Crack Propagation Behavior of Coal Samples from High Gas Seam [J]. Materials, 2022, 15(13): 4500.

[11] XIAO C, HAN D, ZHANG J, et al. Effect of Coal Rank and Coal Facies on Nanopore–Fracture Structure Heterogeneity in Middle-Rank Coal Reservoirs [J]. ACS Omega, 2024, 9(30): 33279-92.

[12] WANG H, TIAN J, WANG J, et al. A novel NMR-capillary pressure method for quantifying pore connectivity and its impact on permeability evolution [J]. Journal of Hydrology, 2025, 660: 133330.

ISSN: 2710-0588

[13] WU J, XIE D, JOUINI M S, et al. INVESTIGATING THE RELATIONSHIP BETWEEN PORE CHARACTERISTICS, FRACTAL DIMENSION, AND PERMEABILITY OF LIMESTONE USING HIGH-PRESSURE MERCURY INTRUSION, SEM ANALYSIS, AND BP NEURAL NETWORK [J]. Fractals, 2024, 32(05): 2450073.

[14] ZHANG S, LIU H, JIN Z, et al. Multifractal Analysis of Pore Structure in Middle- and High-Rank Coal by Mercury Intrusion Porosimetry and Low-Pressure N2 Adsorption [J]. Natural Resources Research, 2021, 30(6): 4565-84.

[15] MA Y. Multiscale Fractal Characterization of Pore Structure for Coal in Different Rank Using Scanning Electron Microscopy and Mercury Intrusion Porosimetry [J]. Processes, 2022, 10(8): 1577.

[16] HAN W, ZHOU G, GAO D, et al. Experimental analysis of the pore structure and fractal characteristics of different metamorphic coal based on mercury intrusion-nitrogen adsorption porosimetry [J]. Powder Technology, 2020, 362: 386-98.

[17] WANG S, CHEN F, YUE S, et al. Multifractal Characterization of Pore Structure of Coals Using Gas Adsorption Experiment and Mercury Intrusion Porosimetry (MIP) [J]. Fractal and Fractional, 2025, 9(3): 183.

[18] TAO G, WANG Z, JIN Y, et al. Multiscale Pore–Fracture Structure Characteristics of Deep Coal Reservoirs in the Eastern Margin of the Ordos Basin, China [J]. Natural Resources Research, 2025, 34(3): 1557-84.

[19] LI Z, REN T, LI X, et al. Multi-scale pore fractal characteristics of differently ranked coal and its impact on gas adsorption [J]. International Journal of Mining Science and Technology, 2023, 33(4): 389-401.

[20] ZHANG N, WANG S, XUN X, et al. Pore Structure and Fractal Characteristics of Coal-Measure Sedimentary Rocks Using Nuclear Magnetic Resonance (NMR) and Mercury Intrusion Porosimetry (MIP) [J]. Energies, 2023, 16(9): 3812.

[21] JIAO L, ANDERSEN P Ø, ZHOU J, et al. Applications of mercury intrusion capillary pressure for pore structures: A review [J]. Capillarity, 2020, 3(4): 62-74.

[22] WEI J, ZHOU X, SHAMIL S, et al. High-pressure mercury intrusion analysis of pore structure in typical lithofacies shale [J]. Energy, 2024, 295: 130879.

[23] MIAO Z, QINJIE L, XINGZHEN W, et al. Multiple fractal characterization of medium-high rank coal integrating mercury intrusion porosimetry, N₂and CO₂ adsorption experiments [J]. Journal of China Coal Society, 2024, 49(5): 2394-404.

[24] HAN L, HUANG D, QIU Z, et al. Pore–Fracture Connectivity of High-Rank Coal in Qinshui Basin, China [J]. Natural Resources Research, 2025, 34(5): 2757-73.

[25] WANG S, CHEN F, YUE S, et al. Multifractal Characterization of Pore Structure of Coals Using Gas Adsorption Experiment and Mercury Intrusion Porosimetry (MIP) [J]. Fractal and Fractional, 2025, 9: 183.

[26] YUE C, QIQI L, DONGMIN M, et al. Combined multi-scale characterization of pores in ultra-thick coal seams of Jurassic Xishanyao Formation, Tiaohu-Malang sags, Santanghu Basin [J]. PETROLEUM GEOLOGY & EXPERIMENT, 2025, 47(1): 104.